IASS 2020/21 SURREY 7
International Conference on Spatial Structures 2020/21

Proceedings of the IASS Annual Symposium 2020/21 and the 7th International Conference on Spatial Structures
Inspiring the Next Generation
23 – 27 August 2021, Guilford, UK
S.A. Behnejad, G.A.R. Parke and O.A. Samavati (eds.)

All glass, compression-dominant polyhedral bridge prototype: form-finding and fabrication

Yao LU[*,a], Matthew CREGAN[b], Philipp A CHHADEH[c], Alireza SEYEDAHMADIAN[d], Mohammad BOLHASSANI[e], Jens SCHNEIDER[c], Joseph R YOST[b], Masoud AKBARZADEH[a,f]

[*,a] Polyhedral Structures Laboratory, School of Design, University of Pennsylvania, Philadelphia, USA
[b] Structural Engineering Teaching and Research Laboratory (SETRL), Villanova University, Villanova, USA
[c] Institute for Structural Mechanics and Design, Technical University of Darmstadt, Darmstadt, Germany
[d] Neoset Designs, New York City, USA
[e] The Bernard and Anne Spitzer School of Architecture, The City College of New York, New York City, USA
[f] General Robotic, Automation, Sensing and Perception (GRASP) Lab , School of Engineering and Applied Science, University of Pennsylvania, Philadelphia, USA

Abstract

The recent development of three-dimensional graphic statics using polyhedral reciprocal diagrams (PGS) has greatly increased the ease of designing complex yet efficient spatial funicular structural forms, where the inherent planarity of the polyhedral geometries can be harnessed for efficient construction processes. Our previous research has shown the feasibility of leveraging this planarity in materializing a 10m-span, double-layer glass bridge made of 1cm glass sheets. This paper presents a smaller bridge prototype with a span of 2.5m to address the larger bridge's challenges regarding form-finding, detail developments, fabrication constraints, and assembly logic. The compression-only prototype is designed for prefabrication as a modular system using PolyFrame for Rhinoceros. Thirteen polyhedral cells of the funicular bridge are materialized in the form of hollow glass units (HGUs) and can be prefabricated and assembled on-site. Each HGU consists of two deck plates and multiple side plates held together using 3M™ Very High Bond (VHB) tape. A male-female glass connection mechanism is developed at the sides of HGUs to interlock each unit with its adjacent cells to prevent sliding. A transparent interface material is placed between the male and female connecting parts to avoid local stress-concentration. This novel construction method significantly simplifies the bridge's assembly on a large scale. The design and construction of this small-scale prototype set the foundation for the future development of the full-scale structure.

Keywords: polyhedral graphic statics, 5-axis waterjet, cast glass, hollow glass unit, funicular structure, form-finding, fabrication

1. Introduction

Geometric structural design methods based on 2D reciprocal diagrams are regarded as a powerful design tool that has been studied and practiced by many designers, engineers, and researchers. The geometric relationship between form and force was initially proposed by Rankine [15], and Maxwell formulated the topological and reciprocal relationship [12] as reciprocal form and force diagrams. In Culmann's book *Die Graphische Statik* [9], the term "graphic statics" (GS) was used for the first time to indicate the design and analysis methods using reciprocal diagrams. GS was then further developed in the following decades by Cremona [8], Bow [7], and many others. It was not only used to analyze forces in a structural form, but also applied in the form-finding of efficient structures by constructing and manipulating the

reciprocal form and force diagrams. Chiasso Shedd (1923-1925) and Salginatobel Bridge (1929) by Robert Maillart are two outstanding examples of utilizing graphic statics to design concrete structures. However, the application of this 2D method in the real world is quite restricted, as the three-dimensional (3D) structures are only extrusions or juxtapositions of the simple 2D design [5].

The recent development of 3D graphic statics greatly increased the ease of designing spatial structures. There are two subcategories in the realm of 3D graphic statics using reciprocal diagrams, vector-based (D'Acunto [10]) and polyhedron-based (Akbarzadeh [3]), and they follow different rules in constructing the form and force 3D dualities. For vector-based 3D graphic statics, a force diagram is "made out of closed cycles of force vectors – also defined as force polygons – in which the lengths of the vectors are equivalent to force magnitudes" [10]. The 3D duality of it can be described as follows, the form edges are mapped to the force edges, the form vertices to cycles for force polygons, the form polygons to force vertices, where form and force polygons are not necessarily planar. In contrast, for the polyhedron-based 3D graphic statics, the force equilibrium is enforced by the closeness of polyhedrons, and the duality is established by mapping form vertices to force polyhedrons, form edges to force faces, form faces to force edges, form polyhedrons to force vertices, where the force magnitude of an edge is equivalent to the area of the corresponding face. In the scope of this paper, PGS will be used to refer to polyhedral graphic statics.

The inherent planarity of the polyhedral geometries can be harnessed for efficient construction processes using sheet materials. Our previous research has shown the feasibility of leveraging this planarity in materializing a 10m-span, double-layer glass bridge made of 1cm glass sheets only [4]. Sheet-based construction system, which uses faces from the form diagram, has several advantages over the frame-based system, which uses the edges. First, sheet-based system offers more stability because it can be considered as a face-stiffened frame. Secondly, the sheet system eliminates the use of spatial nodes, which greatly reduces the complexity of design and fabrication. As a continuation of a previous research, this paper presents the design and fabrication of a 2.5m-span glass bridge prototype (Figure 1), aiming to address the larger bridge's challenges regarding form-finding, detail developments, fabrication constraints, and assembly logic.

2. Design

The design process consists of two stages: form-finding and materialization. In the first stage of form-finding, a double-layer funicular geometry (which has one layer of polyhedron cells) is produced. In the second stage, the polyhedral cells are used as guide geometries to generate the hollow glass units (HGU).

2.1. Form-finding

The major purpose of form-finding is to establish an efficient compression-only form for a design load of 1kN. The reciprocal relationship of the form and force diagram in PGS allows the manipulation of the magnitude of design loads and the topology and geometry of the form. The first step is to construct an initial force diagram which enforces both the equilibrium of external forces, represented as a Global Force Polyhedron (GFP). The equilibrium of internal nodes is then induced by Nodal Force Polyhedrons (NFP) [3][11] that are inside the space of the GFP. Then, the form diagram can be finalized by making use of its geometrical degree of freedom and constraining the vertex location as well as edge length with the help of PolyFrame [14][13] for Rhinoceros [16]. This section breaks down the form-finding process with detailed explanations of the sub-steps.

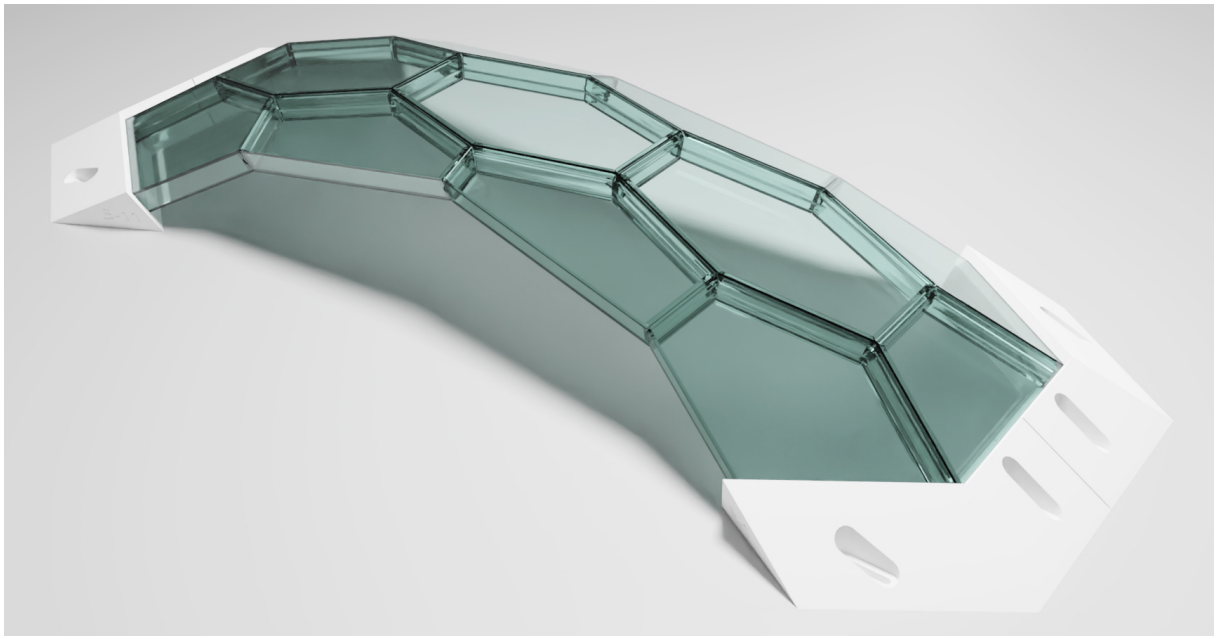

Figure 1: Rendering of the 2.5m-span glass bridge

2.1.1. Form-finding of a single-layer funicular bridge

The form-finding starts with constructing a force diagram of a single-layer funicular bridge. As demonstrated by Akbarzadeh [3], there are two common ways of manipulating force diagrams, aggregating polyhedrons and subdividing polyhedrons, both change the topology and design feature in the derived form diagram. For the 3D funicular shell structures, the common characteristic of their force diagrams is that all the polyhedron cells converge to a point or a line. Base on this characteristic, the force diagram of the glass bridge is made by extruding a 2D aggregation of polygonal faces to a point (Figure 2), where the 2D polygonal faces determine the bridge topology as well as applied load distribution, and the extrusion height determines the bridge rise and internal force magnitudes. The total area of the faces maps to the total applied load of 1kN, and the area of each face maps to the magnitude of the tributary load on the corresponding node. By changing the areas of the polygonal faces, the distribution of the applied load can be manipulated. The derived form diagram with 13 polygonal faces is constrained on 4 anchor points, which controls the span (2.5m) and width (1.3m) of the bridge.

Adjacent edge angles and edge lengths are two extra key geometrical parameters that also need to be tuned in this stage as these are related to the fabrication constraints. More details about the fabrication constraints will be revealed in section 4. The angles between any pair of connecting edges are controlled to be greater than 60 degrees, and the lengths of the internal edges (the edges shared by two polygonal faces) are set to be smaller than 500mm. The edge intersection angles are controlled by adjusting the edge angles of the initial 2D polygons in the force diagram, and the edge lengths can be constrained in the form diagram using PolyFrame.

2.1.2. Double-layer funicular bridge by subdividing force polyhedrons

After having the single-layer funicular form and force diagrams, the double-layer form can be derived by subdividing the force polyhedrons of the single-layer form. Subdivision is a design methodology that can generate a variety of topologically different compression-only forms for a given boundary condition. By subdividing the GFP or the NFPs into smaller closed, convex NFPs, more edges and vertices can be

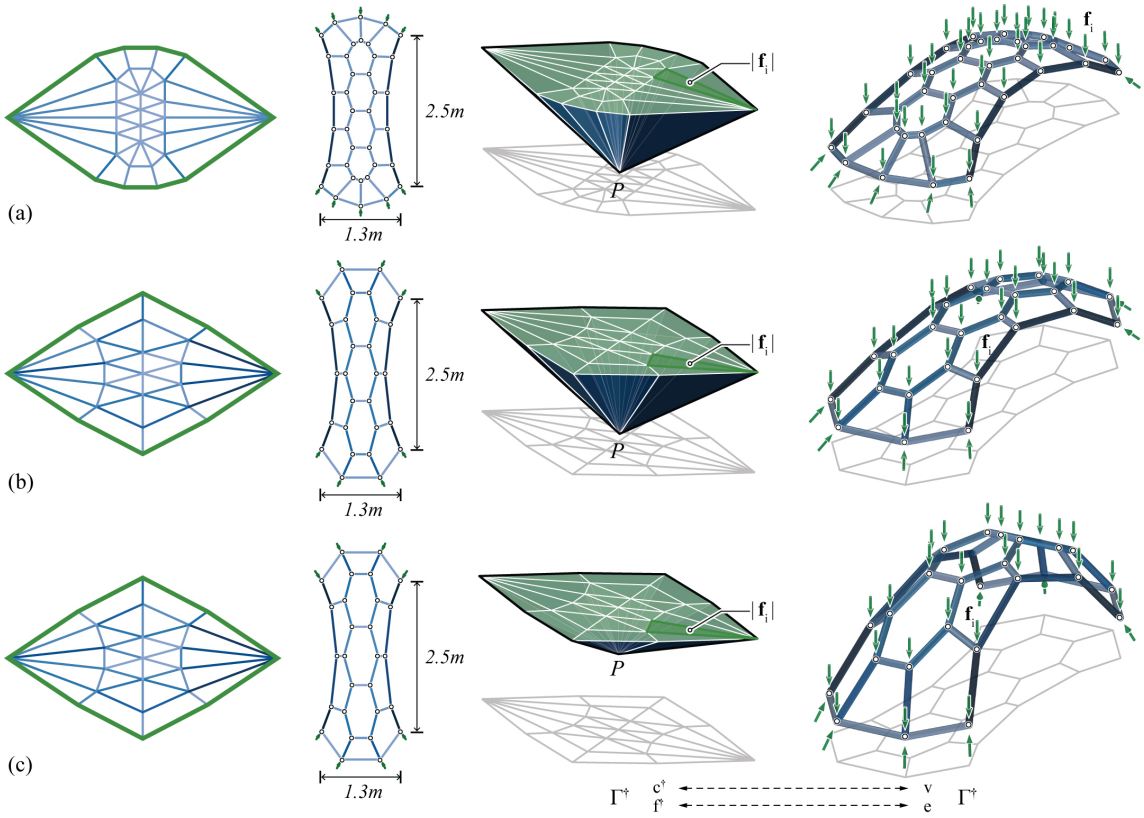

Figure 2: The form-finding of a single-layer bridge form. (a) and (b) have different topologies but the same rise; (b) and (c) have the same topology but different rise.

generated in the form diagram while nodal and global equilibriums are still ensured [1][2].

To transform the funicular form from single-layer to double-layer, all the force polyhedrons are split into two halves from the middle by a surface as illustrated in Figure 3. Afterward, all the faces are planarized to enforce the planarity of the polyhedrons. At this point, all 13 polygonal faces are transformed into polyhedron cells. The curvature of the cutting surface is the key parameter that influences the resulting form, as it is related to the tilting angle of the contact faces of the neighboring cells in the double-layer form (Figure 3). The tilting angles are important because the contact faces better be as perpendicular to the force flow as possible in order to reduce the possibility of local sliding failure. A series of subdivision schemes are developed using various surface curvatures from which an optimal form is selected (Figure 3c). Finally, the edge lengths of the double-layer form are adjusted to make sure every polyhedron cell has a thickness of around 100mm.

2.2. Materialization

The earlier research on the fabrication, assembly, and behavior of a prism HGU shows that it has a good mechanical performance. When designing the small-scale bridge, the same form strategy is followed. Unlike the previous research where only one HGU is investigated, this bridge has multiple HGUs, therefore the contact details between the adjacent HGUs are devised carefully to avoid both local sliding failure and direct glass-to-glass contact. For the modeling process, the half-face data structure (Nejur and Akbarzadeh [14]) of PolyFrame is exploited to facilitate the generation of the detailed model, and a computational model is developed using C#.

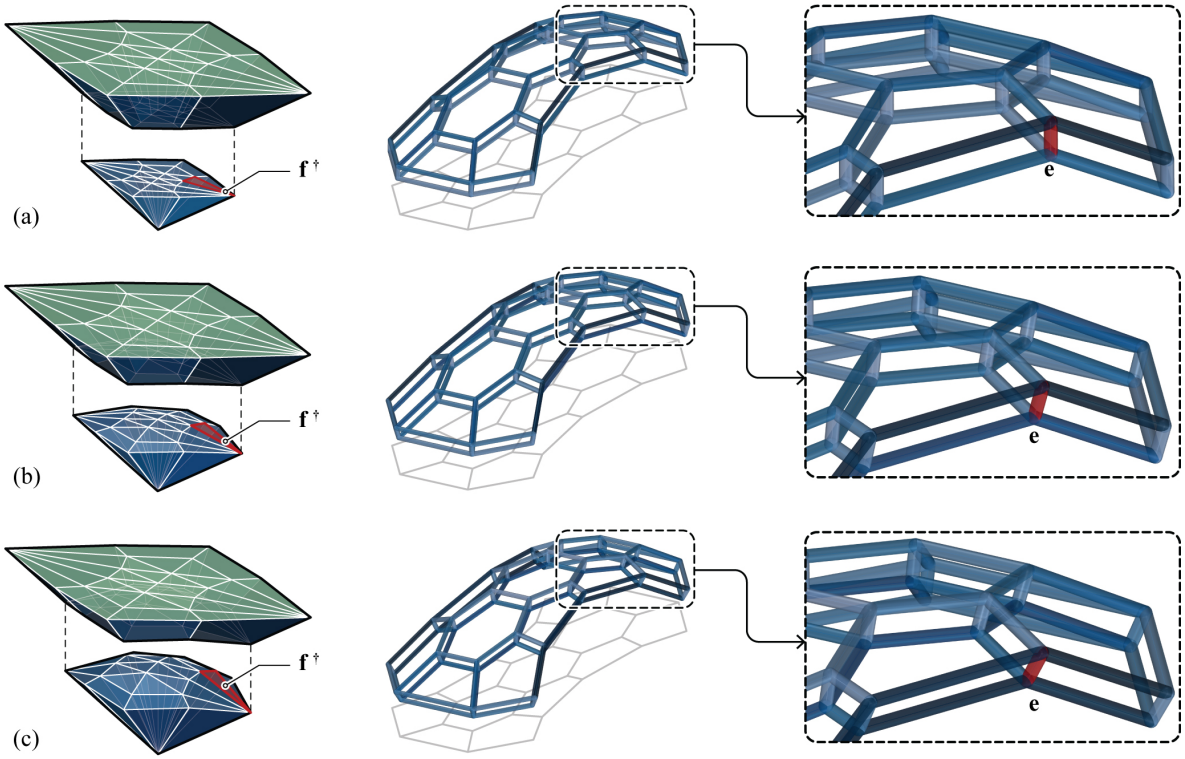

Figure 3: Transform the single-layer form to double-layer by subdividing the force polyhedrons. (a)-(c) show that different angle of the subdividing face changes the edge orientation in the form.

2.2.1. Glass parts: deck plates and side plates

The faces of each of the 13 polyhedron cells are treated differently. Each cell has one top face, one bottom face, and several side faces. Like the earlier research, the top and bottom faces are materialized as deck plates using 9.5mm (3/8 inch) annealed glass as illustrated in Figure 4. For the side faces, however, there are two different categories, one facing the neighbor polyhedron cell and another exposed to the outside. For the side faces that contact the neighboring cells, the side plates with a male-female locking mechanism (Figure 5a) are developed to enforce the connection between the adjacent HGUs, which need thicker and irregular glass. For the other side faces exposed to the outside, since no locking mechanism is needed, the same 9.5mm annealed glass is used.

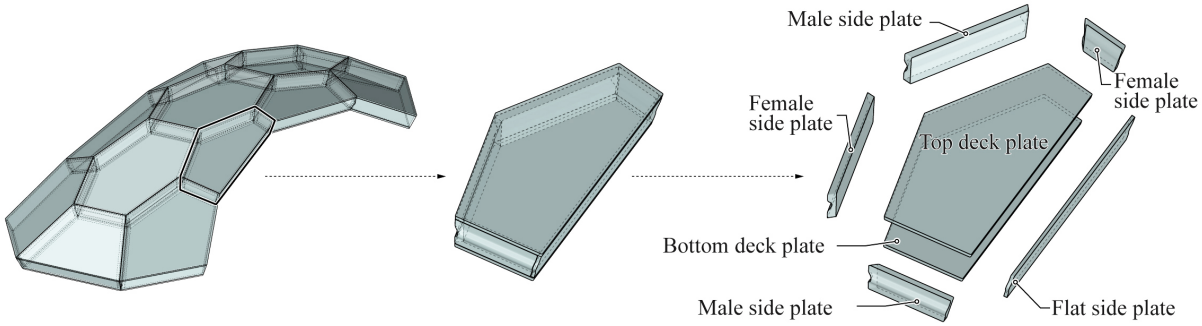

Figure 4: Glass parts in one HGU.

For the side plates with male-female connection, the irregular glass parts have to be customized as there

is no off-the-shelf product available. Kiln casting is chosen to be the fabrication method because it can be accomplished using the University facilities. More information about casting glass will be discussed in section 4. To increase the fabrication and production ease, the profiles of the male and female side plates are standardized so that all the male side plates share the same master shape, and all the female side plates share another master shape (Figure 5b). Therefore, only two molds are needed for kiln casting, the fabrication process is greatly simplified. Since all the internal edges are constrained smaller than 500mm as described in section 2.1.1., thus 500mm in length is sufficient for the cast glass master shapes.

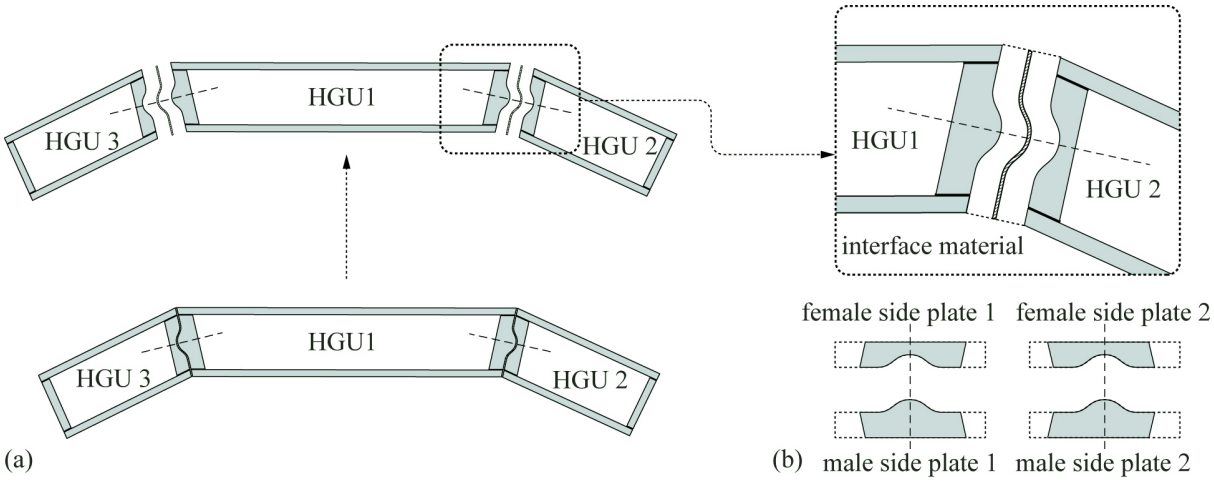

Figure 5: Locking mechanism between adjacent HGUs (a) Bridge cross section, (b) Inter-HGU connection detail.

The individual plate geometric details are illustrated in Figure 6. All the corners are rounded with a 5mm radius fillet, and all side plates are beveled according to the geometry of their neighbors. All the bevels are flat or singly curved and the bevel tilting angles are all within 60 degrees to assure they can be cut with a 5-axis waterjet cutter.

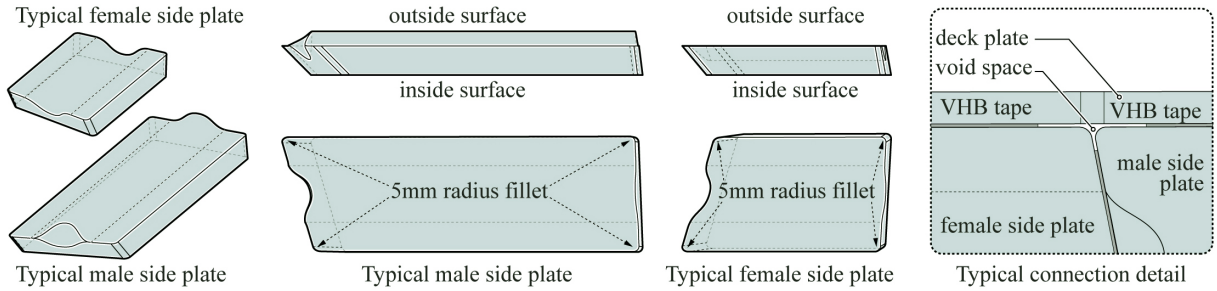

Figure 6: Details of the typical side plate geometry and the typical connection.

2.2.2. Bonding agent: 3M™ Very High Bond (VHB) tape

A gap of 1mm is left between any two glass parts within one HGU where 1mm thick transparent VHB tape is to be applied (Figure 6). VHB tape is a collection of double-sided foam tapes made with an acrylic adhesive and manufactured using closed-cell technology. This soft bonding agent not only holds the glass parts together but also eliminates the glass-to-glass contact within one HGU.

2.2.3. Between HGUs: interface material

Additionally, to eliminate the direct contact and local stress concentration of the glass parts between each pair of the neighboring HGUs, a piece of 3mm (1/8 inch) thick plastic sheets with a lower modulus of

elasticity is placed as interface material (Figure 5a and 5b). The shape of the interface material complies with the shape and curvature of the male-female connecting surfaces.

3. Investigation of the structural performance

Before starting fabrication of the full-scale 10m span bridge, a small-scale model experiment is carried out to investigate the structural performance of the 2.5m-span bridge. Since the form of the bridge is designed based on one specific load case, its behaviors under other load cases need to be examined. The main objective of the small-scale model experiment is to see how the modular system of HGU works under different loading scenarios, so each HGU is appropriately simplified and printed as a hollow block using Polylactic Acid (PLA) filament at 1:5 scale. The total self-weight of the 13 printed blocks is 780g, and this is recorded for comparison with the applied load. Support of the bridge is also 3D printed with PLA and fixed onto a piece of 13mm (1/2 inch) thick plywood using bolts. The bolt holes of the support have extra space along the span direction, which allows for adjustment of the distance between the support and makes sure the printed blocks can be tightly held together. After assembly of the small-scale model, it is then loaded with steel weights. Four load cases are tested: symmetric concentrated load, symmetric tributary load, asymmetric concentrated load, and asymmetric tributary load (Figure 7). The buckling load and the greatest relative displacement between the blocks are recorded. The test result shows that the bridge buckles most from a concentrated-asymmetric load. In all cases, the bridge model successfully bears an applied load of more than 15 times its self-weight. In the symmetric-distributed load case, the total load equals 25.64 times its self-weight. However, it is noted, that although the model is not buckling in some load cases, the relative displacements between the adjacent HGUs are significant. This may be due to the accumulated 3D printing and assembly error, or the low self-weight of the bridge. This scaled model test shows a good potential of the load-bearing capacity, and the more rigorous structural performance study awaits further efforts.

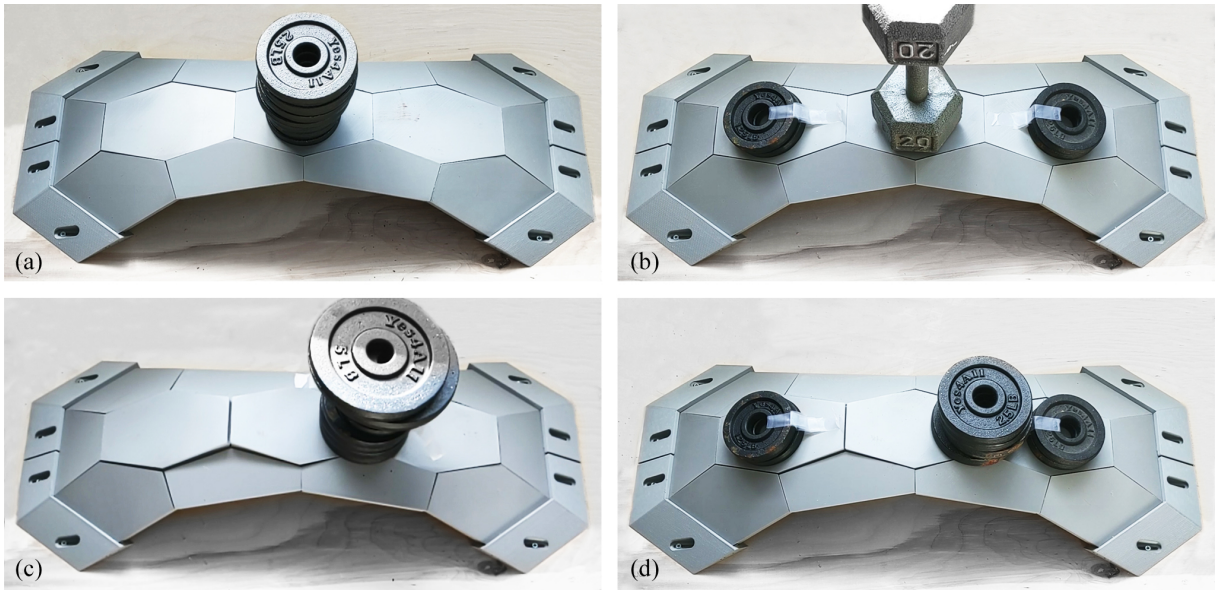

Figure 7: Loading scenarios of the small-scale model experiment. (a) symmetrical concentrated (b) symmetrical tributary (c) asymmetrical concentrated (d) asymmetrical tributary.

To further analyze the structural performance of the full-scale bridge, a Finite Element Analysis is needed and will be performed in future research. This will give us a more precise simulation of the structural

behavior under different load cases.

4. Fabrication and assembly of one HGU

One HGU from the bridge is chosen to explore the fabrication and assembly methodology. The experience gained and errors found in this trial assembly will help to adjust workflow in the ultimate fabrication and assembly of the small-scale bridge.

4.1. Glass preparation

As mentioned in section 2.2.1, 9.5mm (3/8in) glass will be used for the deck plates and flat side plates and they can be purchased from the vendor, but the irregular glass for the male or female side plates needs to be kiln cast. Two sets of one-time molds are developed using silica and plaster, and 1inch thick float glass is used as the cast material (Figure 8a). Each round of kiln cast takes about 48 hours, and a bigger mold is made to facilitate the production speed, which can make 4 pairs of male and female master shapes in one cast as showed in Figure 8b.

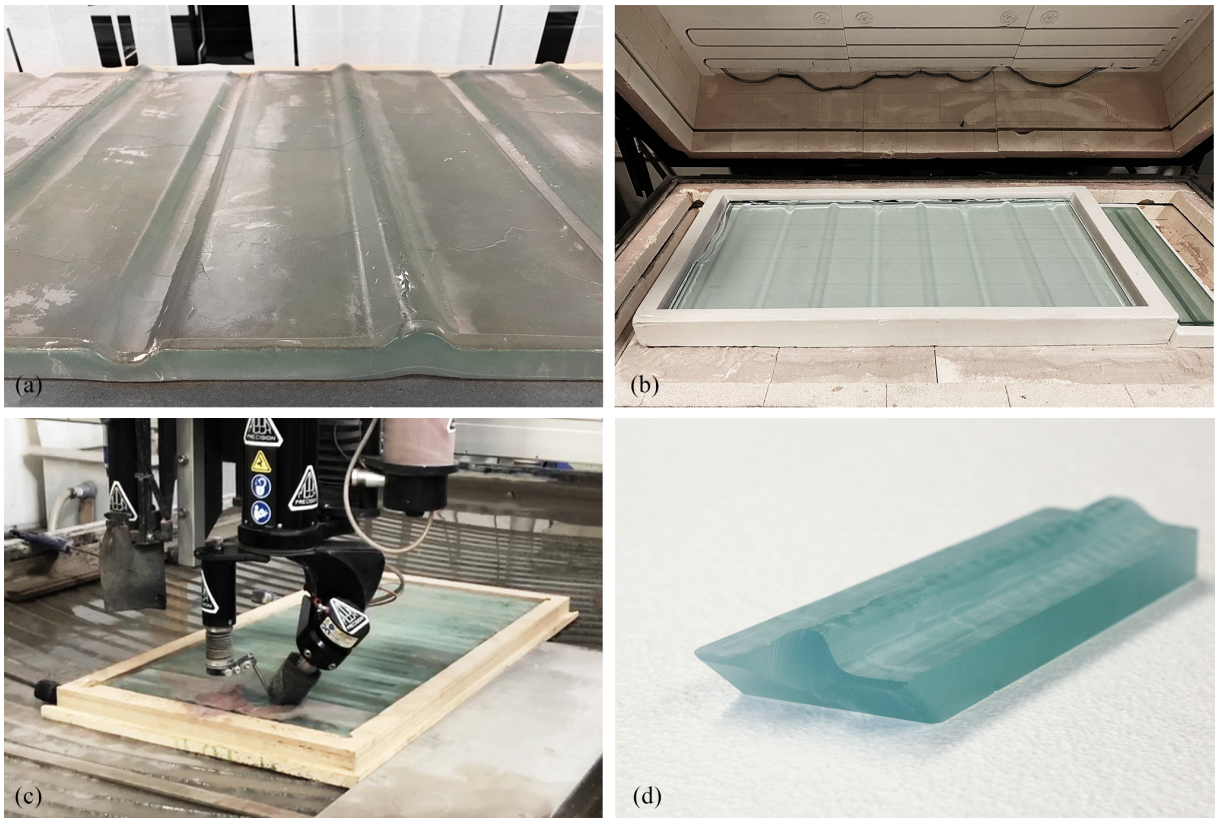

Figure 8: Kiln-cast glass and waterjet cutting. (a) Cast glass, (b) mold and kiln, (c) 5-axis abrasive waterjet, (d) the edge cuts of a male side plate.

4.2. Waterjet

A 5-axis abrasive waterjet is used to cut the glass into desired shapes (Figure 8c). There is a limit of the cutting angle being 60 degrees from vertical. In the actual fabrication, it is better to keep all the angles below 59.5 degrees to get a precise result. This fabrication constraint is considered during the design stage and all the cut angles are carefully examined to ensure they all below the limit. Besides, the top surface of the glass needs to be flat for the waterjet cutting head to rest on, so a fixture is made for the

cast glass which allows them to be cut with the topology facing down. Figure 8d shows the edge cuts of a typical male side plate. The total setup and cutting time for this HGU is around 3 hours.

4.3. Assembly of one HGU

Special connection clips (Figure 9a) and bars (Figure 9b) are devised to true the assembly to the required geometric tolerance. The connection clips are 3D printed using PLA, and the connection bars are cut with a CNC router out of a 6mm high-density polyethylene (HDPE) sheet. A labeling system is also developed to help place the connection clips and bars. All labels are embedded into the connection parts during the fabrication.

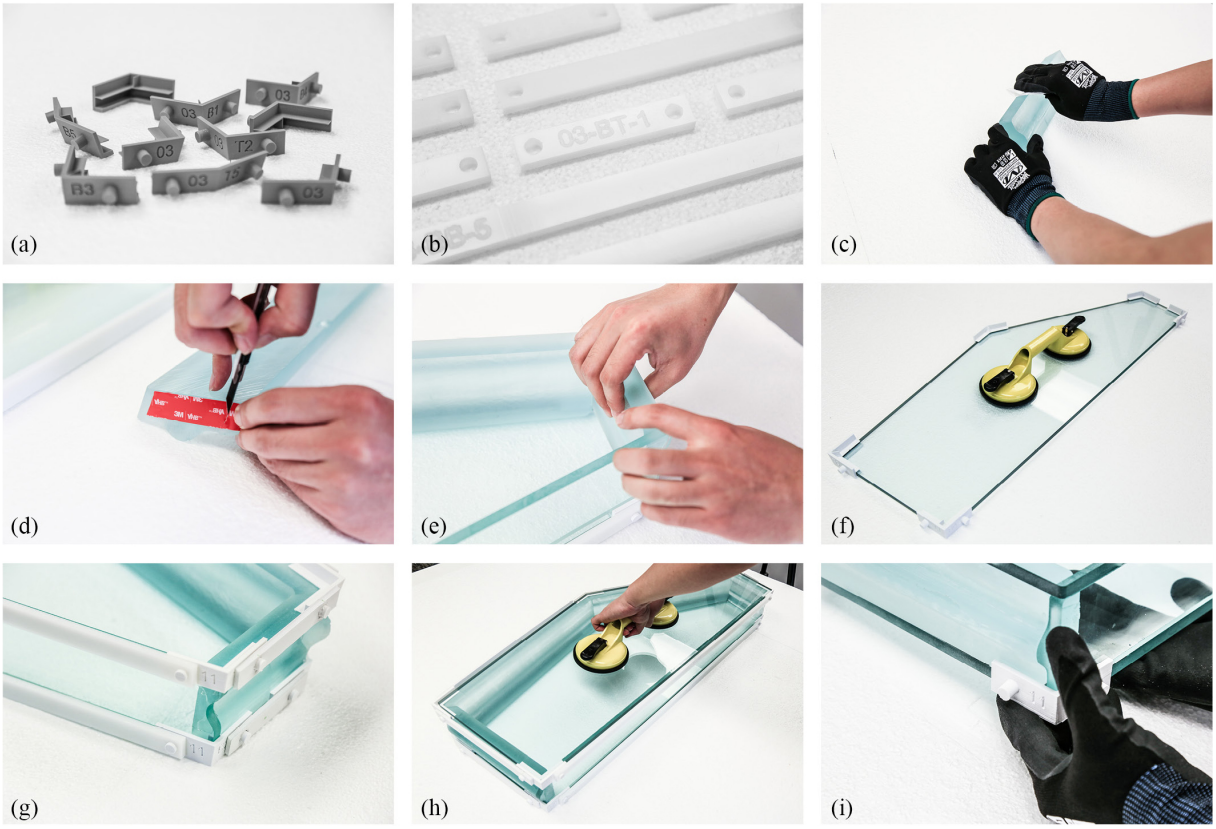

Figure 9: (a)-(i) Assembly process of one HGU.

Before the assembly, all the glass parts are cleaned using a 50% isopropyl alcohol 50% water solution and lint-free cloth (Figure 9c). The assembly starts with connecting the side plates. During this step, the VHB tape is first applied to the short dimensions of each side plate, with one tape side bonded to the glass bevel and the other side still with the protective film. At this point, if the tape is wider than the attached surface then it will be trimmed using a razor blade to match the shape of the glass bevel (Figure 9d). The protective foil was then removed, and all the side plates are bonded to form a cycle (Figure 9e). This is then followed by attaching them to the bottom deck plate. The bottom connection clips and bars are first put in place around the bottom deck plate, and this will ensure the required bottom shape of the side plates is achieved when assembled (Figure 9f). The top shape is ensured by the top connection clips and bars (Figure 9g). VHB tape is applied to the bottom side of the side plate cycle, and all top connection clips and bars together with the side plate cycle are lowered down to the bottom deck plate. The placement of the top deck plate starts with applying VHB tape to the top surface of the side plate cycle. Later, the top deck plate is lowered down and bonded to the VHB tape with the help of suction

lifters (Figure 9h). All the connection clips and bars are then removed completing the assembly process (Figure 9i). Lastly, to secure the VHB bonding, the recommended pressure of 100kPa is applied to the edges of the deck plates using dimensional wood blocking and clamps. The fully assembled HGU and the detail of a typical male and female side plates connection are shown in Figure 10. At the end the size of HGU here will be the same as the full scale specimen that was built and tested in the earlier part of this research [6].

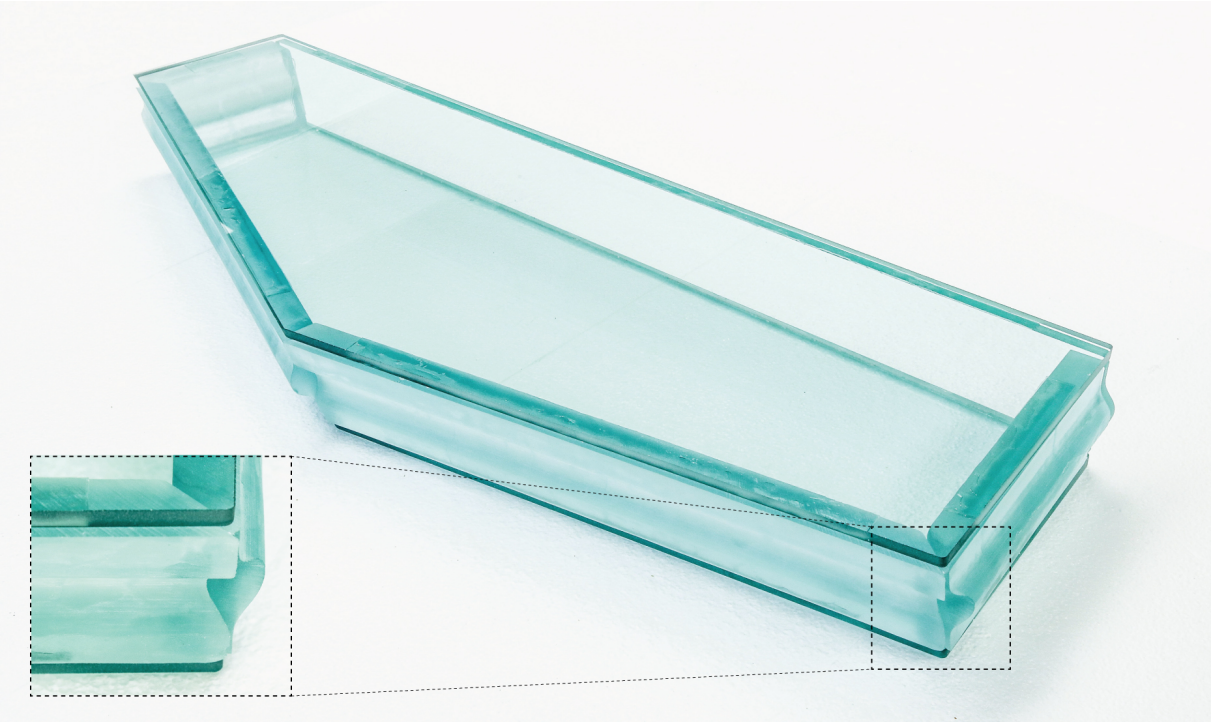

Figure 10: The fully assembled HGU.

5. Conclusion and future work

This paper introduces the design and fabrication of a 2.5m span bridge made with prefabricated HGUs. 3DGS method of analysis is used during the compression-only form-finding procedure, and a computational model is made for the efficient generation of the geometric details. A series of physical prototype tests are performed on the bridge design to understand the mechanical behavior under different load cases. The scaled model test shows the potential to bear more than 15 times its self-weight. One HGU from the bridge is then selected to explore the fabrication and assembly methodology. The efficient fabrication and assembly of the HGU demonstrates the feasibility of using HGUs as a modular and prefabricated construction system. In future work, a Finite Element Analysis is required to simulate the structural performance of the full-scale bridge. The fabrication of all HGUs and the assembly and construction of the whole bridge will be continued. Further loading experiments on the small-scale bridge are then required to examine the actual structural behavior of the 2.5m-span glass bridge.

6. Acknowledgment

This research was partially funded by University of Pennsylvania Research Foundation Grant (URF) and National Science Foundation CAREER Award to Masoud Akbarzadeh (NSF CAREER-1944691 CMMI). It was also funded by Villanova University Summer Grant Program (USG).

References

[1] M. Akbarzadeh, T. Van Mele, and P. Block. Compression-only form finding through finite subdivision of the force polygon. In *Proceedings of International Association for Shell and Spatial Structures (IASS) Symposium*, volume 16, pages 1–7, 2014.

[2] M. Akbarzadeh, T. Van Mele, and P. Block. Three-dimensional compression form finding through subdivision. In *"Proceedings of the International Association for Shell and Spatial Structures (IASS) Symposium"*, volume 21, pages 1–7, 2015.

[3] Masoud Akbarzadeh. *3D Graphical Statics Using Reciprocal Polyhedral Diagrams*. PhD thesis, ETH Zurich, 2016.

[4] Masoud Akbarzadeh, Mohammad Bolhassani, Andrei Nejur, Joseph Robert Yost, Cory Byrnes, Jens Schneider, Ulrich Knaack, and Chris Borg Costanzi. The Design of an Ultra-Transparent Funicular Glass Structure. pages 405–413, April 2019. Publisher: American Society of Civil Engineers.

[5] L.L. Beghini, J. Carrion, A. Beghini, A. Mazurek, and W.F. Baker. Structural optimization using graphic statics. *Structural and Multidisciplinary optimization*, 49(3):351–366, 2014.

[6] Mohammad Bolhassani, Cory Byrnes, Joseph Robert Yost, Jens Schneider, and Andrei Nejur. Behavior of Modular Components in a Funicular Glass Bridge. In *IASS Annual Symposium 2019 - Structural Membranes 2019-Form and Force*, Barcelona, Spain, October 2019.

[7] Robert H. Bow. *Economics of Construction in Relation to Framed Structures*. Cambridge Library Collection - Technology. Cambridge University Press, 2014.

[8] L. Cremona. *Graphical statics: two treatises on the graphical calculus and reciprocal figures in graphical statics. Translated by Thomas Hudson Beare*. Clarendon Press, Oxford, 1890.

[9] K. Culmann. *Die Graphische Statik*. Verlag Meyer und Zeller, Zürich, 1864.

[10] Pierluigi D'Acunto, Jean-Philippe Jasienski, Patrick Ole Ohlbrock, Corentin Fivet, Joseph Schwartz, and Denis Zastavni. Vector-based 3D graphic statics: A framework for the design of spatial structures based on the relation between form and forces. *International Journal of Solids and Structures*, 167:58–70, August 2019.

[11] Juney Lee, Tom VAN Mele, and Philippe Block. Form-finding explorations through geometric transformations and modifications of force polyhedrons. page 10, 2016.

[12] J. Clerk Maxwell. I.—On Reciprocal Figures, Frames, and Diagrams of Forces. *Earth and Environmental Science Transactions of The Royal Society of Edinburgh*, 26(1):1–40, 1870. Publisher: Royal Society of Edinburgh Scotland Foundation.

[13] Andrei Nejur and Masoud Akbarzadeh. Polyframe beta: A geometry-based structural form-finding plugin for Rhinoceros 3D.

[14] Andrei Nejur and Masoud Akbarzadeh. PolyFrame, Efficient Computation for 3D Graphic Statics. *Computer-Aided Design*, 134:103003, May 2021.

[15] W. J. M. Rankine. XVII. Principle of the equilibrium of polyhedral frames.

[16] Robert McNeel Associates. Rhinoceros 6.0.